

## Size dependence of surface cluster models: CO adsorbed on Cu(100)

Klaus Hermann,\* Paul S. Bagus, and Constance J. Nelin<sup>†</sup>  
IBM Almaden Research Laboratory, San Jose, California 95120-6099

(Received 10 October 1986)

We have studied the strong variation of cluster-model binding energies of the CO/Cu(100) adsorbate system for clusters with between 1 and 34 atoms to represent the Cu surface. Based on the constrained space orbital variation approach the metal-CO interaction is decomposed into three terms: (1) charge superposition of the free CO and metal subunits, (2) charge polarization within the subunits, and (3) charge transfer between the subunits. The results show that one can identify bonding contributions which vary slowly with cluster size and shape. Further, relations between the cluster representation of the Cu(100) conduction band and the metal-CO bond strength can be established. These relations make it possible to determine the importance of cluster artifacts for the metal-CO bonding from electronic properties of the bare metal cluster. Our results provide further support for the validity of using clusters with small numbers of substrate atoms to describe chemisorption on metal surfaces.

## I. INTRODUCTION

The molecular-orbital (MO) cluster model has been used quite extensively to study various properties of atomic<sup>1</sup> and molecular<sup>2</sup> adsorbates on surfaces; for a review of early work in this area see also Ref. 3. In this model, the solid surface is represented by a cluster of a few, typically up to 30, substrate atoms. Adsorbates, atoms or molecules, are added to the substrate cluster and MO wave functions for this system are used to determine properties of the adsorbate-substrate interaction. In most cases only a single adsorbate is considered. Clearly, this approach treats most effectively those contributions to the adsorbate-substrate interaction which are due to local changes in the substrate electronic structure. Thus, it is reasonable to expect that the cluster model can be successful in describing the behavior of covalently bonded adsorbates, e.g., CO, where the local chemical bonding is dominant. We have also shown that the cluster model can treat important aspects of systems where the Coulomb interaction between adsorbate and substrate dominates.<sup>4-7</sup>

A major concern in adsorbate cluster-model studies is the dependence of properties on the number of substrate atoms in the cluster. As a result of rapid increase in computational effort with cluster size only very few systematic studies of the cluster size dependence<sup>8-12</sup> have been carried out. As a general result of these studies, one finds that size dependence is closely connected to the particular physical property under consideration. While some of the properties, e.g., vibrations of the adsorbate<sup>12,13</sup> and photoemission binding-energy shifts,<sup>14-16</sup> converge fairly rapidly with cluster size to those of a real surface, others are specific to the particular cluster. In particular, the adsorbate binding energy to metal substrate clusters, especially for covalently bonded systems, generally show very strong oscillations for the range of cluster sizes that have been treated with *ab initio* methods.

In our previous studies of the metal-CO interaction,<sup>11,17-20</sup> we have analyzed the bonding and deter-

mined the individual importance of intraunit polarization and interunit donation charge rearrangements. In particular, we have shown that there are three dominant contributions. First, there is a large repulsion when the charge distributions of the separated metal and CO units are superimposed. Second, polarization of the metal charge reduces this repulsion, and, third, metal-to-CO  $2\pi^*$  backdonation makes the most important contribution to the covalent metal-CO bonding. In this work, we elucidate the origin of the CO binding variation with cluster size for the CO/Cu(100) system represented by  $\text{Cu}_n\text{CO}$  clusters with  $n=1, 5, 10, 14,$  and  $34$  Cu atoms. We show that the origin of the strong variation of the adsorbate binding energy with cluster size is mainly due to variations of electrostatic effects when the charge densities of the adsorbate and substrate are superimposed; for CO, this electrostatic interaction is repulsive. There are also variations of the substrate polarization which reduce this repulsion. The substrate polarization increases monotonically with the amount of charge superposition; however, the polarization only offsets part of the superposition. In contrast, energy contributions from adsorbate (CO) polarization and donation between the components characterizing local bonding effects depend much less strongly on cluster size. Our analysis shows that the local interaction and bonding of adsorbates on surfaces are represented quite well, albeit often qualitatively rather than quantitatively, by self-consistent-field (SCF) wave functions for clusters with a small number of metal atoms.

Further, the binding-energy contributions due to electrostatic effects of the adsorbate-substrate charge superposition depend strongly on the charge density of the substrate cluster near the adsorbate. This density is mainly determined by the energetically highest occupied substrate orbitals, those close to the cluster Fermi level. It is found that repulsion at the initial charge-superposition step is increased if substrate valence orbitals of  $\sigma$  character are among the most diffuse ones (weakening the CO-metal bonding). Further, the CO-metal bonding is increased by

$\pi$ -type Cu valence orbitals being close to the substrate Fermi level. This explains why the CO-Cu<sub>n</sub> interaction is repulsive for  $n=1, 10$ , and 34 Cu atoms while it is attractive for Cu<sub>5</sub>CO and Cu<sub>14</sub>CO.

For the bare Cu<sub>n</sub> and the Cu<sub>n</sub>CO clusters, we have computed SCF wave functions. Electron correlation effects, not included in the SCF wave function, increase the importance of the  $2\pi^*$  backdonation somewhat.<sup>20,21</sup> The CO-metal interaction energy for SCF wave functions is modestly smaller than for correlated wave functions and the SCF value of the equilibrium metal-CO distance is slightly longer. For example, correlated, configuration-interaction (CI) wave functions for the Cu<sub>5</sub>CO cluster<sup>21</sup> give a binding energy 0.27 eV larger and a bond distance 0.2 bohr shorter than the SCF value. Despite these relatively small quantitative changes, the general features of the interaction are very similar for both SCF and correlated wave functions.<sup>20</sup> Thus, for the present purpose of comparing the interaction of CO with different size Cu<sub>n</sub> clusters, SCF wave functions are adequate. We have used the constrained space orbital variation (CSOV) analysis<sup>17,18</sup> to characterize the bonding. With this analysis, we are able to decompose the CO-Cu<sub>n</sub> binding energy into various contributions coming from polarization of the adsorbate and substrate or donation between the two components. As a result, electrostatic and polarization contributions are found to be important. Among charge-transfer (donation) contributions,  $\pi$ -electron transfer from the metal to CO, usually referred to as  $\pi$  backbonding, turns out to be energetically more important than  $\sigma$ -electron transfer from CO to the metal ( $\sigma$  bonding) in contrast to the traditional Blyholder scheme.<sup>18</sup> Finally, we note that we have not considered the coupling, or embedding, of our clusters to the remainder of the surface environment.<sup>19</sup> This embedding is commonly neglected.

Section II reviews the details of the calculations and gives the basic ideas of the CSOV method while Sec. III discusses the numerical results. Finally, the conclusions are summarized in Sec. IV.

## II. COMPUTATIONAL DETAILS

We consider Cu<sub>n</sub> and Cu<sub>n</sub>CO clusters with  $n=1, 5, 10, 14$ , and 34 as models to study the interaction of CO with the Cu(100) surface. The geometries of the  $n > 1$  clusters are chosen to represent sections of bulk Cu near the surface and are kept fixed at the bulk geometry;<sup>24</sup> the Cu-Cu nearest-neighbor distance is  $d_{\text{Cu-Cu}} = 2.54$  Å. In the following we use the notation Cu<sub>n</sub>( $p_1, p_2, \dots$ ) to specify the number of Cu atoms of the first, second, etc., surfaces layers included in the cluster. In Cu<sub>n</sub>CO, CO was assumed to approach a singly coordinated on top-site with its molecular axis perpendicular to the surface. The C-O and Cu-C distances used were near the equilibrium geometry determined from low-energy electron diffraction (LEED) measurements<sup>25</sup> and near the calculated SCF equilibrium values for the Cu<sub>5</sub>CO and Cu<sub>14</sub>CO clusters. Figure 1 shows the geometry of the Cu<sub>34</sub>CO which is the largest cluster considered here. The smaller clusters are all subsystems of Cu<sub>34</sub>CO.

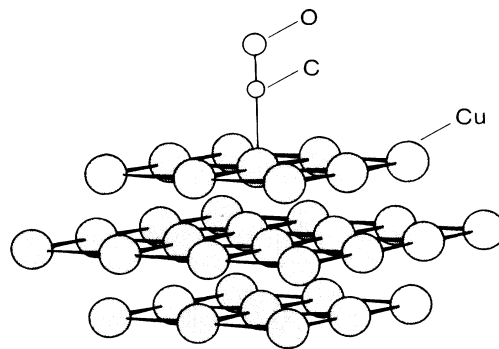


FIG. 1. Schematic representation of the Cu<sub>34</sub>CO cluster. The smaller clusters, Cu<sub>1</sub>(1,0,0)CO, Cu<sub>5</sub>(1,4,0)CO, Cu<sub>10</sub>(5,4,1)CO, and Cu<sub>14</sub>(5,4,5)CO, are formed from Cu<sub>34</sub>(9,16,9)CO by removing, from each layer, the Cu atoms which are most distant from CO and retaining those which are closest.

The electronic states of the clusters are calculated with the *ab initio* SCF linear combination of atomic orbitals (LCAO) method<sup>26</sup> using flexible all-electron basis sets of contracted Gaussian-type orbitals, (CGTO's), for the central Cu atom in Cu<sub>n</sub> and for C and O in Cu<sub>n</sub>CO. The Cu basis set is taken from Wachter's optimization<sup>27</sup> for the free atom and includes two CGTO's to represent Cu 4*p* character; a diffuse *d* function as recommended by Hay<sup>28</sup> has also been added. The complete Cu basis set has 8*s*,6*p*,4*d* CGTO's contracted from 14*s*,11*p*,6*d* functions. The C and O basis sets are 4*s*,3*p* contractions of the van Duijneveldt<sup>29</sup> 9*s*,5*p* primitive set. The Cu atoms surrounding the central Cu in Cu<sub>n</sub>CO are treated in an approximate way by replacing their Ar + 3*d*<sup>10</sup> cores with pseudopotentials,<sup>17</sup> and only the 4*sp* electrons contributing to the conduction band are explicitly included in the cluster wave function. These environmental Cu atoms are not directly involved in the dative covalent bonding of Cu(100) to CO. Details of the pseudopotential and basis-set parameters are given elsewhere.<sup>17,30</sup>

The use of pseudopotentials for the environment Cu atoms does not introduce artifacts into the cluster wave functions. This has been verified by comparing cluster calculations using pseudopotentials for the environmental Cu atoms to calculations where all 29 electrons for each Cu atom are explicitly included. For Cu<sub>5</sub>(1,4)CO, the Cu-C equilibrium separation obtained from a full all-electron calculation differs by only 0.02 bohr and the CO-metal binding energy by only 0.03 eV compared to the pseudopotential treatment.<sup>30</sup> Further, for CO interacting with (planar) Cu<sub>5</sub>(5,0) at a Cu-C distance,  $d_{\text{Cu-C}} = 3.70$  bohr, close to the values obtained from LEED data<sup>25</sup> and from CI wave functions<sup>21</sup> for Cu<sub>5</sub>CO, the (repulsive) interaction also differs by only 0.03 eV between the full all-electron and the pseudopotential treatment. Thus, the differences between the all-electron treatment and that using pseudopotentials for the environmental atoms are extremely small.

The binding between CO and the metal clusters is analyzed by the CSOV method.<sup>17,18</sup> This method makes it possible to determine the energetic importance of dif-

ferent contributions to the interaction between an adsorbed molecule and a cluster. Its basic ideas will be discussed briefly. A CSOV step is defined as the self-consistent solution of the  $N$ -electron equations for a system denoted  $AB$  consisting of two subunits,  $A$  and  $B$ . For our present application,  $A$  is the adsorbed molecule and  $B$  is the metal-atom cluster  $\text{Cu}_n$ . Two boundary conditions are imposed at each CSOV step. First, the charge density of one of the components is fixed at a given density. Second, the variational space of the other component is constrained on the basis of physical principles. To use this for the analysis of the interaction between  $A$  and  $B$ , one calculates a sequence of CSOV steps with different boundary conditions.

The starting point is the superposition of the charge densities of the two separate components at the geometry of the combined system. A comparison of the respective total energy with that of the two separate components yields an interaction energy representing the purely electrostatic effect of superposition. In the first CSOV step, one keeps the charge density of the adsorbed molecule  $A$  fixed in its free state and solves the variational equations for the cluster  $B$  in the variational space of the cluster basis functions. Physically, this describes the polarization of the cluster in the presence of the frozen molecule. In the second CSOV step, the variational space of the cluster orbitals is increased by including the virtual, unoccupied orbitals of the molecule and charge transfer and dative covalent bonding from the cluster to the molecule is possible. This charge transfer can be split into different symmetry contributions of the virtual space. In the third CSOV step one freezes the charge distribution of the cluster from the previous step and solves the variational equations for the molecule in the space of the molecular basis functions. This accounts for polarization of the molecule in the presence of the frozen cluster. Finally, in the fourth step virtual orbitals of the cluster are included in the variational space which allows for charge transfer from the molecule to the cluster.

It is important to emphasize that the order in which these constrained variations are performed does not have a large effect. Test calculations with the orbitals of the molecule varied first followed by the cluster variation have shown that the contribution of a given CSOV step is essentially the same as for the order described above. The present CSOV approach is restricted to systems where the

covalent bonding is dative. If open shells of the adsorbate of the cluster are involved in the bonding extensions must be made.<sup>5,20</sup>

In order to account for the interplay between different CSOV steps, it may be necessary to continue the above sequence iteratively. In the systems considered, this was not necessary and only one sequence was used. The main virtue of the analysis lies in the fact that one can calculate the total energy of the combined system of adsorbate and substrate at each CSOV step. Therefore, one can determine the energy contributions of different physical effects, polarization and charge transfer, to the total binding energy and make quantitative statements about the relative importance of these effects for the molecule-cluster interaction.

### III. RESULTS AND DISCUSSION

First, we consider briefly the character of the SCF ground states of the bare  $\text{Cu}_n$ ,  $n=1, 5, 10, 14$ , and  $34$ , clusters. The symmetry of these clusters can be described by the point group  $C_{4v}$  and the cluster orbitals and configurations will be denoted according to the irreducible representations of  $C_{4v}$ . For each cluster, the central, adsorption-site Cu atom contributes 11 electrons (10  $3d$  and 1  $4sp$ ) to the high-lying cluster orbitals while the environmental Cu atoms each contribute one electron ( $4sp$ ) to the "conduction" band. Although there is a limited mixing of  $d$  and  $4sp$  character in the high-lying  $\text{Cu}_n$  cluster orbitals, they are dominantly of one type or the other. The total symmetry and the ground-state configuration of the clusters are given in Table I.

Figure 2 shows energy-level diagrams of the  $\text{Cu}_n$  clusters where the levels refer to SCF orbital energies  $\epsilon$  of the occupied  $sp$  (solid lines) and  $d$  (dashed lines) orbitals. For all cases, the  $d$  "band" is very narrow. This is a consequence of using a pseudopotential which includes the  $d$  shells of the environmental atoms in their cores. As a result the cluster  $d$  orbitals are localized on the central Cu atom. The orbital energies of the  $d$  levels are  $\sim 13$  eV below vacuum which suggests considerably larger  $d$ -level binding than obtained from photoemission<sup>31</sup> or from band calculations.<sup>32</sup> This is because the SCF Koopmans's-theorem ionization potentials (IP's) given by the  $\epsilon$ 's shown in Fig. 2, do not include final-state relaxation,<sup>29,30</sup> which is expected to be large for localized  $d$  levels. The widths

TABLE I. Electronic configurations for the  $\text{Cu}_n$  and  $\text{Cu}_n\text{CO}$  clusters and the SCF interaction energies  $E_{\text{int}}(\text{SCF})$ , in eV, between  $\text{Cu}_n$  and CO. The bond distances are  $d_{\text{Cu-C}}=3.70$  and  $d_{\text{C-O}}=2.15$  bohr. Negative  $E_{\text{int}}$  values indicate repulsion between CO and  $\text{Cu}_n$ .

$n$	State	Configuration $\text{Cu}_n$	Configuration $\text{Cu}_n\text{CO}$	$E_{\text{int}}(\text{SCF})$
1	$^2A_1(^2S)$	$7a_1^1 1b_1^2 1b_2^2 3e^4$	$12a_1^1 1b_1^2 1b_2^2 4e^4$	-0.55
5	$^2E$	$7a_1^2 1b_1^2 1b_2^2 4e^3$	$12a_1^2 1b_1^2 1b_2^2 5e^3$	0.45
10	$^1A_1$	$8a_1^2 1b_1^2 2b_2^2 4e^4$	$13a_1^2 1b_1^2 2b_2^2 5e^4$	-0.40
14	$^1A_1$	$8a_1^2 1b_1^2 2b_2^2 5e^4$	$13a_1^2 1b_1^2 2b_2^2 6e^4$	0.28
34	$^1A_1$	$11a_1^2 4b_1^2 2b_2^2 7e^4$	$16a_1^2 4b_1^2 2b_2^2 8e^4$	-0.55

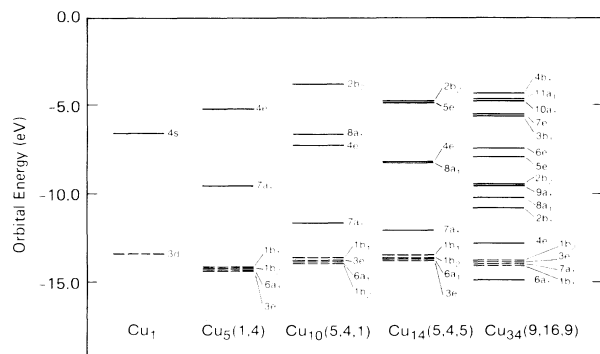


FIG. 2. Valence level diagrams of the  $\text{Cu}_n$  substrate clusters,  $n=1,5,10,14,34$ . The levels are labeled according to the irreducible representation of the  $C_{4v}$  symmetry group. Levels of dominant  $d$  character are marked by a dashed line.

of the  $sp$  levels, “ $sp$  band,” are 7.8, 7.1, and 10.5 eV for the larger clusters,  $\text{Cu}_{10}$ ,  $\text{Cu}_{14}$ , and  $\text{Cu}_{34}$ , respectively. This is compared to the  $\sim 8$ -eV width of the occupied part of the  $4sp$  band given by band-structure calculations.<sup>28</sup> For these clusters, the highest occupied orbital has an  $\epsilon \sim 4$  eV below vacuum, a value comparable to the  $\text{Cu}(100)$  work function of  $\sim 4.4$  eV.<sup>31</sup>

The  $sp$  “conduction-band” cluster orbitals are delocalized over all the atoms in the cluster and final-state relaxation energies will be small for these levels. For the relatively small  $\text{Cu}_5$  cluster, for example, the relaxation energy for ionization to the ground state of  $\text{Cu}_5^+$  is 0.3 eV. Thus, the  $sp$  conduction-band orbital energies for the occupied orbitals of the cluster do provide a useful guide to the band width and position which is consistent with studies of bulk Cu (Ref. 32). However, there is a major difference among the various  $\text{Cu}_n$  clusters in the ordering of the higher orbitals of the  $sp$  conduction band; this difference involves the point-group symmetry,  $a_1, a_2, e, b_1, b_2$ , of these orbitals. Of these representations, the  $a_2$ ,  $b_1$ , and  $b_2$  have nodal properties such that they cannot contain  $s$  or  $p$  character from the central, adsorption site, Cu atom. On the other hand, the  $a_1$  and  $e$  levels can and do contain adsorption site Cu atom  $s$  and/or  $p$  character. These are the  $C_{4v}$  representations which map, for the on top site, onto the  $\sigma(a_1)$  and  $\pi(e)$  representations of the CO molecule. Thus, the  $a_1$  and  $e$  conduction-band orbitals will be involved in the dative metal-CO interaction. For  $\text{Cu}_5$  and  $\text{Cu}_{14}$ , the highest  $e$  orbital is well above the highest  $a_1$  orbital; the reverse ordering,  $a_1$  above  $e$ , occurs for the  $\text{Cu}_{10}$  and  $\text{Cu}_{34}$  clusters. We shall show below that this ordering is important for the absolute magnitude of the bond strength between  $\text{Cu}_n$  and CO.

When CO is added to the on top site of the central atom to form  $\text{Cu}_n\text{CO}$  as a model for  $\text{CO}/\text{Cu}(100)$ , the ground-state configuration is found to be given by that of  $\text{Cu}_n$  plus the five  $a_1(\sigma)$  and one  $e(\pi)$  orbitals of the CO ground state  $1\Sigma^+(5\sigma^2 1\pi^4)$ . The major property of concern for this work is the SCF interaction energy,  $E_{\text{int}}(\text{SCF})$ , given by

$$E_{\text{int}}(\text{SCF}) = E_{\text{tot}}(\text{Cu}_n) + E_{\text{tot}}(\text{CO}) - E_{\text{tot}}(\text{Cu}_n\text{CO}; \text{SCF}), \quad (1)$$

where  $E_{\text{tot}}(X)$  denotes the SCF total energy of system  $X$ . (For  $\text{Cu}_n\text{CO}$ , we include in  $E_{\text{tot}}$  the notation SCF to distinguish it from total energies of the  $\text{Cu}_n\text{CO}$  at various CSOV steps, discussed later on.) With the definition of Eq. (1), positive  $E_{\text{int}}$  values indicate an attractive interaction while negative values indicate repulsion. For the  $\text{Cu}_n\text{CO}$  clusters, we give, in Table I, the configurations and the values of  $E_{\text{int}}(\text{SCF})$  for  $d_{\text{Cu-C}} = 3.70$  and  $d_{\text{C-O}} = 2.15$  bohr. These bond distances are close to the measured equilibrium distances.<sup>25</sup> The interaction for  $\text{Cu}_1\text{CO}$ ,  $\text{Cu}_{10}\text{CO}$ , and  $\text{Cu}_{34}\text{CO}$ , is repulsive by 0.55, 0.40, and 0.55 eV, respectively. For  $\text{Cu}_1\text{CO}$  and  $\text{Cu}_{10}\text{CO}$ , we have examined several Cu-C distances and determined that the interaction is repulsive at *all* distances. We also expect to find an overall repulsive interaction curve for  $\text{Cu}_{34}\text{CO}$ . For  $\text{Cu}_5\text{CO}$  and  $\text{Cu}_{14}\text{CO}$  the interaction between  $\text{Cu}_n$  and CO is attractive by 0.45 and 0.28 eV, respectively. These surprisingly large variations of the interaction energies compared to relatively small differences in cluster size can be understood from CSOV analyses for the clusters. In Fig. 3, we plot the interaction energies of the dif-

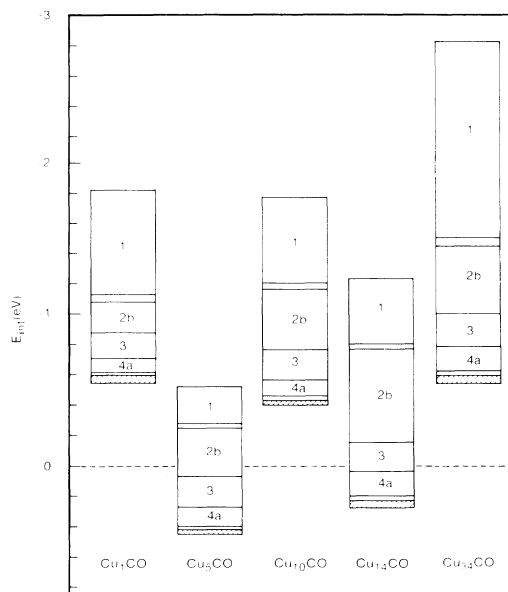


FIG. 3. Block diagrams representing the CSOV decomposition of the interaction energy  $E_{\text{int}}$  for the  $\text{Cu}_1\text{CO}$  to  $\text{Cu}_{34}\text{CO}$  clusters. The top of the block for each cluster indicates the value of  $E_{\text{int}}$  for the superposed charge distributions of the  $\text{Cu}_n$  and CO subunits. The bottom of each block indicates the value of  $E_{\text{int}}$  for the full, unconstrained, SCF wave function and the hatched areas indicate the differences between the final CSOV step  $4b$  result and the full SCF. CSOV steps  $2a$ , Cu to CO  $\sigma$  backdonation, and  $4b$ , CO to Cu  $\pi$  donation, make too small a contribution for the blocks to be numbered. The bond distances are  $d_{\text{Cu-C}} = 3.70$  and  $d_{\text{C-O}} = 2.15$  bohr.

ferent CSOV steps,  $N_{\text{CSOV}}, E_{\text{int}}(\text{Cu}_n\text{CO}; N_{\text{CSOV}})$  as block diagrams. The CSOV  $E_{\text{int}}$  is defined similarly to  $E_{\text{int}}(\text{SCF})$ , Eq. (1), as

$$E_{\text{int}}(\text{Cu}_n\text{CO}; N_{\text{CSOV}}) = E_{\text{tot}}(\text{Cu}_n) + E_{\text{tot}}(\text{CO}) - E_{\text{tot}}(\text{Cu}_n\text{CO}; N_{\text{CSOV}}), \quad (2)$$

where  $E_{\text{tot}}(\text{Cu}_n\text{CO}; N_{\text{CSOV}})$  is the total energy of  $\text{Cu}_n\text{CO}$  at the respective CSOV step  $N_{\text{CSOV}}$ .

The electrostatic interaction of the charge superposition of CO and  $\text{Cu}_n$  represented by the top of each block in Fig. 3 shows repulsion in all cases. However, the repulsion energies vary substantially between the clusters with  $\text{Cu}_5\text{CO}$  yielding the smallest ( $-0.52$  eV) and  $\text{Cu}_{34}\text{CO}$  the largest value ( $-2.80$  eV). The actual magnitude of the charge-superposition repulsion is found to be connected with the electronic structure of the bare substrate clusters. The charge-superposition repulsion arises from the overlap and interpenetration of the unperturbed, frozen,  $\text{Cu}_n$  and CO charge distributions.<sup>19</sup> As noted above, the  $a_2$ ,  $b_1$  and  $b_2$  symmetry orbitals of  $\text{Cu}_n$  do not contain any central Cu atom  $s$  or  $p$  character and therefore cannot contribute significantly to the overlap and interpenetration of CO and  $\text{Cu}_n$ . This will arise principally from the  $a_1$  and  $e$  orbitals. The CO orbital contributing most to the repulsion is the  $5\sigma$  lone pair which is directed towards the metal surface. The  $4\sigma$  CO orbital is concentrated principally at the O end of the molecule further from the surface. The centers of charge of the C-O bonding  $1\pi$  and  $3\sigma$  orbitals are located between C and O with higher charge concentration on O than on C. Thus, the  $\text{Cu}_n$  orbitals of dominant importance for the charge-superposition repulsion are those of  $a_1$  symmetry. An inspection of the valence levels in Fig. 2 shows that the higher-lying  $a_1$  levels of  $\text{Cu}_1$ ,  $\text{Cu}_{10}$ , and  $\text{Cu}_{34}$  are energetically close to the cluster Fermi energy  $E_F$  defined as the energy of the highest occupied cluster level. This is in contrast to  $\text{Cu}_5$  and  $\text{Cu}_{14}$  where the highest  $a_1$  levels are further from  $E_F$ , 4.4, and 3.4 eV, respectively. As a consequence, the  $\text{Cu}_n$  cluster electron density in the surface region near the CO molecule is smaller in  $\text{Cu}_5$  and  $\text{Cu}_{14}$  than in  $\text{Cu}_1$ ,  $\text{Cu}_{10}$ , and  $\text{Cu}_{34}$ . This effect, which can be visualized in respective density contour plots, determines the charge overlap with CO and results in a much smaller charge-superposition repulsion for  $\text{Cu}_5\text{CO}$  and  $\text{Cu}_{14}\text{CO}$  compared to  $\text{Cu}_1\text{CO}$ ,  $\text{Cu}_{10}\text{CO}$ , and  $\text{Cu}_{34}\text{CO}$ .

The charge-superposition repulsion in  $\text{Cu}_n\text{CO}$  is reduced in the first CSOV step by 0.2–1.3 eV due to polarization of the substrate.<sup>17</sup> In addition, this polarization contribution becomes larger as the charge-superposition repulsion increases. This is simply due to the fact that an increased charge-superposition repulsion reflects an increased perturbation acting on the substrate cluster which leads to a stronger reaction of the substrate. Electron transfer from  $\text{Cu}_n$  to CO included in the second CSOV step increases the interaction energy by 0.25–0.65 eV. This contribution can be split into electron transfer of  $\sigma(a_1)$  symmetry, step 2a, and  $\pi(e)$  symmetry, step 2b. It is obvious from the diagrams of Fig. 3 that, in all clusters, the dominant contribution originates from  $\pi$  electron

transfer from  $\text{Cu}_n$  to CO. Part of the  $\pi$  backdonation originates from the metal  $d\pi$  orbitals and part comes from the  $p\pi(e)$  orbitals in the “conduction band.”<sup>35</sup> A rough measure of the importance of the  $d\pi$  contribution to the backdonation is given by the size of block 2b for  $\text{Cu}_1\text{CO}$ . Since  $\text{Cu}_1$  has no  $4p\pi$  character, the change in  $E_{\text{int}}$  is entirely due to the  $d\pi$  charge transfer and covalent bonding to CO. If we exclude  $\text{Cu}_5\text{CO}$ , we can relate the magnitude of the conduction-band contribution to block 2b to the position of the  $\text{Cu}_n$  cluster  $e$  levels with respect to the cluster Fermi level. The  $4sp$   $e$  level in the small  $\text{Cu}_5$  cluster is an open shell which contains only 3 electrons, see Table I, while the highest  $e$  levels in the larger clusters are closed shells containing 4 electrons. For  $\text{Cu}_{14}$ , the  $5e$  level is only 0.01 eV below the Fermi level and the  $\pi$  backdonation is largest  $\sim 0.6$  eV. For  $\text{Cu}_{34}$ , the highest  $e$  level is 1.1 eV below the cluster Fermi level resulting in a reduced  $\pi$  backdonation of  $\sim 0.4$  eV. Finally, the  $\pi$  backdonation contribution is slightly smaller for  $\text{Cu}_{10}\text{CO}$  where for  $\text{Cu}_{10}$ , the highest  $e$  level is over 3 eV below the Fermi level.

The interaction energy is further increased by polarization of the CO subunit in the third CSOV step. The energy gain of 0.2 eV is almost independent of cluster size. The fourth CSOV step describing charge transfer from CO to the metal increases the interaction by 0.1–0.2 eV. A subdivision of this CSOV step into  $\sigma$  and  $\pi$  contributions, steps 4a and 4b, respectively, shows that the charge transfer is dominated by CO  $\sigma$  electron donation which is, in all cases, smaller than metal  $\pi$  backdonation. This order of the importance of  $\sigma$  donation and  $\pi$  backdonation has also been found for  $sp$  metals<sup>11</sup> and for transition metals where the  $d\sigma$  levels are not fully occupied and CO  $5\sigma$  to metal  $d$  donation is possible.<sup>36</sup> The fourth CSOV step is found to be rather close to the fully self-consistent result without any constraints which defines the bottom of each block diagram of Fig. 3. The difference is always below 0.05 eV demonstrating that the first CSOV sequence is sufficient to describe the interaction and that there is little interaction between the metal and ligand charge rearrangements. For  $\text{Cu}_{10}\text{CO}$  and  $\text{Cu}_{34}\text{CO}$ , we have performed a second cycle of CSOV variations<sup>36</sup> and found that allowing the metal to polarize in the presence of the rearranged CO accounted for the major part,  $\sim 80\%$ , of the 0.05 eV difference from the full SCF at the end of the first CSOV cycle. Similar results have been obtained for  $\text{Al}_n\text{CO}$  cluster models.<sup>11,37</sup>

The CSOV analyses for all clusters have shown that there are two different types of contributions to the metal-CO bonding. Electrostatic and polarization contributions which are not related to interunit charge transfer or to interunit covalent bonding are important. Among interunit contributions,  $\pi$  electron backdonation from the metal to CO is energetically more important than  $\sigma$  electron donation from CO to the metal. These conclusions which are obtained from the detailed, quantitative CSOV analysis do not agree with the traditional<sup>22</sup> molecular-orbital analysis of carbonyl bonding which describes the bonding entirely in terms of  $\sigma$  donation and  $\pi$  backdonation and neglects the role of polarization. Further,  $\sigma$  donation and  $\pi$  backdonation are placed on an equal foot-

ing with the  $\sigma$  donation possibly being more important. We have shown that the reverse is true. For a comparison of these two points of view see Refs. 38 and 39. Our view of the importance of intraunit polarization as well as interunit charge transfer has also made it possible to understand the photoemission binding-energy shifts<sup>14,15</sup> and the vibrational shifts<sup>12,40,41</sup> observed for chemisorbed molecules.

Further, the electrostatic and substrate polarization contributions depend rather strongly on cluster size and geometry (cf. Fig. 3) and determine to a major degree the actual size of the total binding energy. In contrast, charge transfer and adsorbate polarization are much less dependent on cluster size. Of these effects, the metal to CO  $\pi$  backdonation has the strongest dependence on the particular substrate cluster. This allows us to understand why the metal-CO interaction is attractive for Cu<sub>5</sub>CO and Cu<sub>14</sub>CO while it is repulsive for Cu<sub>1</sub>CO, Cu<sub>10</sub>CO, and Cu<sub>34</sub>CO.

It is important to consider the magnitude of the changes in the Cu-CO binding energy and equilibrium bond distance which arise when correlation effects are included. For Cu<sub>5</sub>CO, CI wave functions have been obtained<sup>21</sup> which include single and double excitations from the higher-lying occupied cluster orbitals of  $e(\pi)$  symmetry into the unoccupied, virtual  $e(\pi)$  orbitals. These excitations should account for the most important correlation effects of the Cu-CO bonding since our CSOV analysis shows that  $\pi$  backdonation makes the dominant contribution to interunit bonding. This has been verified by more extensive CI calculations for Cu<sub>5</sub>CO and Cu<sub>10</sub>CO which have included  $a_1(\sigma)$  as well as  $e(\pi)$  orbitals.<sup>42</sup> For Cu<sub>5</sub>CO, the  $e(\pi)$  electron CI wave function for  $d_{\text{Cu-C}}=3.70$  bohr gives  $E_{\text{int}}=0.73$  eV which is 0.27 eV larger than the SCF  $E_{\text{int}}=0.45$  eV. A large part of the correlation contribution to  $E_{\text{int}}$ ,  $\geq 50\%$ , arises from the involvement of the localized Cu  $3d\pi$  orbital in the backdonation and dative bonding. This is shown by correlated results<sup>20</sup> for Cu<sub>1</sub>CO where the Cu  $3d\pi$  orbital makes the only contribution to the backdonation. Similar CI contributions to the Cu-CO binding energy have been obtained<sup>42</sup> for Cu<sub>10</sub>CO suggesting that even larger clusters would show a correlation effect of similar magnitude. Thus, an estimate for the correlation energy contribution to the binding energy for CO/Cu(100) is 0.25–0.30 eV, which is a significant fraction of the 0.6–0.7 eV binding energy for CO/Cu(100) at an on-top site.<sup>43</sup> As a consequence, the SCF binding energy will be positive (attractive) and  $\sim 0.3$  eV for the surface system. The SCF interaction curves for Cu<sub>5</sub>CO and Cu<sub>14</sub>CO give CO-metal binding energies of 0.45 and 0.27 eV, respectively (see Table I). Further, the Cu-CO equilibrium distance obtained from SCF wave functions for Cu<sub>5</sub>CO and Cu<sub>14</sub>CO is 3.9 bohr. This is close to the experimental result, 3.7 bohr, and hence a good estimate of the bond distance. The Cu-CO equilibrium distance obtained from CI wave functions<sup>21</sup> for Cu<sub>5</sub>CO, 3.69 bohr, is in excellent agreement with experiment. These results suggest strongly that SCF wave functions for suitably chosen small clusters lead to binding energies and bond distances which are in qualitative but not fully quantitative agreement with experiment.<sup>25,43</sup>

#### IV. CONCLUSIONS

In this study, we have analyzed the interaction of CO with Cu<sub>n</sub>CO cluster models,  $n=1, 5, 10, 14,$  and  $34,$  representing the CO/Cu(100) adsorbate system. From CSOV analyses on these systems we confirm the CO-metal binding picture proposed earlier<sup>17</sup> which demonstrates the importance of electrostatic and polarization contributions. Further, among charge-transfer (donation) contributions,  $\pi$  electron transfer from the metal to CO,  $\pi$  backdonation, is energetically more important than  $\sigma$  electron transfer from CO to the metal. This is consistent with the interpretation of CO adsorbate photoemission spectra,<sup>14,15</sup> and with the vibrational shifts of chemisorbed CO.<sup>12,40,41</sup>

Most importantly, we have identified the origin of the strong variation of the CO-metal binding energy as arising largely from variations in the electrostatic charge superposition and substrate polarization contributions. These contributions depend strongly on cluster size and geometry which are reflected in the substrate cluster electronic energy levels. On the other hand, the more local part of the interaction which includes the metal to CO  $\pi$  backdonation and, in particular, the CO intraunit polarization and  $\sigma$  donation vary much less with cluster size.

We have established relations between the electronic structure of the bare Cu<sub>n</sub> cluster and its interaction with CO. If the high-lying bare cluster levels of  $\sigma(a_1)$  symmetry are near the cluster Fermi level there will be a large electrostatic charge superposition repulsion with CO which is only partly balanced by the substrate polarization. This behavior leads, in the cases we have examined, to a net repulsive interaction. On the other hand, if the high-lying  $\sigma(a_1)$  levels are far from the Fermi level, the net repulsion from the charge superposition is much smaller and including the other charge rearrangements leads to an attractive interaction. Further, if the cluster conduction-band  $\pi(e)$  levels are near the Fermi level, the  $\pi$  backdonation to CO is larger.

This understanding is important for several reasons. First, it establishes the validity of the cluster description of the character of the metal-CO chemisorption bond. Second, it makes it possible to predict from the distribution of levels in the bare cluster conduction band whether its interaction with CO will be attractive or repulsive. This is important when sites other than on top site are examined. For CO chemisorption at an on-top site, the metal to CO bond distance is often known from experiment; see for example, Ref. 25 for bond distances of CO/Ni(100) and CO/Cu(100). One can therefore place CO at the known bond distance and determine various properties even if the SCF cluster binding energy is negative. However, for CO adsorbed at sites different from the on-top site, independent information about the bond distance is usually not available. In these cases, theoretical estimates may provide the only information about surface-adsorbate bond distances. The understanding of cluster size effects developed in this paper leads to criteria for choosing suitable clusters for making these estimates. We believe that our results, including these criteria are of a general nature and apply to adsorbate-metal systems other than CO/Cu(100).

## ACKNOWLEDGMENTS

We express our appreciation to M. R. Philpott for useful discussions. One of us (K.H.) received support from Sonderforschungsbereich 126.

\*Permanent address: Institut für Theoretische Physik, Technische Universität Clausthal, Clausthal, West Germany.

†Permanent address: Analatom Incorporated, 1977 Concourse Drive, San Jose, CA 95131-1708.

<sup>1</sup>For a recent example considering chlorine adsorption see Ref. 5.

<sup>2</sup>For representative examples comparing chemisorption of CO, NH<sub>3</sub>, and PF<sub>3</sub>, see Ref. 14.

<sup>3</sup>K. Hermann, Phys. Bl. **36**, 227 (1980).

<sup>4</sup>P. S. Bagus, in *Plasma Synthesis and Etching of Electronic Materials*, edited by R. T. H. Chang and B. Abeles, Proceedings of the Materials Research Society Symposia (Materials Research Society, Pittsburgh, 1985), Vol. 38, p. 179.

<sup>5</sup>L. G. M. Petterson and P. S. Bagus, Phys. Rev. Lett. **56**, 500 (1986).

<sup>6</sup>K. Hermann, W. Müller, and P. S. Bagus, J. Electron Spectrosc. Relat. Phenom. **39**, 107 (1986).

<sup>7</sup>P. S. Bagus, C. J. Nelin, W. Müller, M. R. Philpott, and H. Seki, Phys. Rev. Lett. **58**, 559 (1987).

<sup>8</sup>K. Hermann and P. S. Bagus, Phys. Rev. B **17**, 4082 (1978).

<sup>9</sup>T. B. Grimley and E. E. Mola, J. Phys. C **9**, 4082 (1978).

<sup>10</sup>C. W. Bauschlicher, P. S. Bagus, and H. F. Schaefer III, IBM J. Res. Dev. **22**, 213 (1978).

<sup>11</sup>K. Hermann, H. J. Hass, and P. S. Bagus, Z. Phys. D **3**, 159 (1986).

<sup>12</sup>P. S. Bagus and W. Müller, Chem. Phys. Lett. **115**, 540 (1985).

<sup>13</sup>K. Hermann, P. S. Bagus, and C. W. Bauschlicher, Phys. Rev. B **30**, 7313 (1984).

<sup>14</sup>P. S. Bagus and K. Hermann, Appl. Surf. Sci. **22/23**, 444 (1985).

<sup>15</sup>P. S. Bagus and K. Hermann, Phys. Rev. B **33**, 2987 (1986).

<sup>16</sup>P. S. Bagus, C. J. Nelin, and K. Hermann, Aust. J. Phys. **39**, 731 (1986).

<sup>17</sup>P. S. Bagus, K. Hermann, and C. W. Bauschlicher, J. Chem. Phys. **81**, 1966 (1984).

<sup>18</sup>P. S. Bagus, K. Hermann, and C. W. Bauschlicher, J. Chem. Phys. **80**, 4378 (1984).

<sup>19</sup>P. S. Bagus, C. J. Nelin, and C. W. Bauschlicher, Phys. Rev. B **28**, 5423 (1983).

<sup>20</sup>C. W. Bauschlicher, P. S. Bagus, C. J. Nelin, and B. O. Roos, J. Chem. Phys. **85**, 354 (1986).

<sup>21</sup>W. Müller and P. S. Bagus, J. Vac. Sci. Technol. A (to be published).

lished).

<sup>22</sup>G. Blyholder, J. Phys. Chem. **68**, 2772 (1964).

<sup>23</sup>The embedding problem has been treated, e.g., by C. R. Fischer and J. B. Witten, Phys. Rev. B **30**, 6821 (1984).

<sup>24</sup>R. G. Wyckoff, *Crystal Structures*, 2nd ed. (Interscience, New York, 1964).

<sup>25</sup>S. Andersson and J. B. Pendry, Phys. Rev. Lett. **43**, 363 (1979); M. Passler, A. Ignatiev, F. Jona, D. W. Jepsen, and P. M. Marcus, *ibid.* **43**, 360 (1979).

<sup>26</sup>The MOLECULE-ALCHEMY program package implemented at the IBM Almaden Research Center, San Jose was used to obtain electronic wave functions for the clusters.

<sup>27</sup>A. J. H. Wachters, J. Chem. Phys. **52**, 1033 (1970).

<sup>28</sup>P. J. Hay, J. Chem. Phys. **66**, 4377 (1977).

<sup>29</sup>F. B. van Duijneveldt, IBM Research Report No. RJ 945, 1971 (unpublished).

<sup>30</sup>P. S. Bagus, C. B. Bauschlicher, C. J. Nelin, B. C. Laskowski, and M. Seel, J. Chem. Phys. **81**, 3594 (1984). The *p*-type Gaussian basis functions used for the pseudopotential atoms are somewhat different in the present work.

<sup>31</sup>J. E. Demuth and D. E. Eastman, Solid State Commun. **18**, 1497 (1976).

<sup>32</sup>See, e.g., V. L. Moruzzi, J. F. Janak, and A. R. Williams, *Calculated Electronic Properties of Metals* (Pergamon, New York, 1978).

<sup>33</sup>K. Hermann and P. S. Bagus, Phys. Rev. B **16**, 4195 (1977).

<sup>34</sup>P. S. Bagus, Phys. Rev. **139**, A619 (1965).

<sup>35</sup>P. S. Bagus, C. J. Nelin, and C. W. Bauschlicher, J. Vac. Sci. Technol. A **2**, 905 (1984).

<sup>36</sup>C. W. Bauschlicher and P. S. Bagus, J. Chem. Phys. **82**, 5889 (1985).

<sup>37</sup>K. Hermann and H. J. Hass (unpublished).

<sup>38</sup>A. E. Wimmer, C. L. Fu, and A. J. Freeman, Phys. Rev. Lett. **55**, 2618 (1985).

<sup>39</sup>P. S. Bagus, K. Hermann, W. Müller, and C. J. Nelin, Phys. Rev. Lett. **57**, 1496 (1986).

<sup>40</sup>W. Müller and P. S. Bagus, J. Vac. Sci. Technol. A **3**, 1623 (1985); J. Electron Spectrosc. Relat. Phenom. **38**, 103 (1986).

<sup>41</sup>K. Hermann, C. J. Nelin, and P. S. Bagus (unpublished).

<sup>42</sup>W. Müller and P. S. Bagus (unpublished).

<sup>43</sup>J. C. Tracy, J. Chem. Phys. **56**, 2748 (1972).